

The Study of the Effect of Coal Feeding Pattern on Combustion Efficiency in Pulverized Coal Combustion using CFD Technique

Wanwilai K. Evans

Department of Chemical Engineering, Faculty of Engineering, King Mongkut's Institute of Technology Ladkrabang, Chalokkrung 1, Ladkrabang, Bangkok, 10520, Thailand, tel. +668 69998908, fax: +662 3298360
wanwilai.ev@kmitl.ac.th

The study of the combustion and thermal flow of a pulverized coal combustion furnace was investigated. Three types of bituminous coal were fed into the combustion chamber without mixing. These coals were different in components, physical and chemical properties, which causes non-uniform combustion. Of interest is how to feed these different types of coal into the furnace. The aim of this work is to study the effect of the feeding pattern on the combustion efficiency using a computational fluid dynamics (CFD) technique, FLUENT 12, a commercial CFD code. The Finite Volume Method (FVM) was applied and the turbulence was modelled by the realizable $k-\varepsilon$ model. The effects of the feeding pattern on combustion efficiency were carried out. Six examples of coal feeding patterns with equivalent coal feed rate were simulated. It was found that feeding coal with a higher fixed carbon content at the top position yielded higher thermal efficiency and also released minimum flue gases (SO_2 , CO_2).

1. Introduction

Coal combustion is one of the most common energy sources, and continues to be so due to its availability and ease of operation. The optimisation operation can reduce pollution emission and enhance the thermal efficiency of combustion. In general, different types of coal will be blended before being fed into the furnace to obtain a uniform feed property. However, in a power station that has a limited area for blending such as the power plant located on reclaimed land in the Gulf of Thailand, several types of coal are fed into the furnace without blending. This could cause an inefficient combustion and increase pollution emissions. Wen et al. (2017) studied the effect of volatile matter composition and chemical reaction mechanisms on pulverized coal combustion characteristics and reported that the combustion characteristics can be significantly affected by volatile matter composition. Therefore, the study of feeding various types of coal to the combustion furnace without blending is beneficial. CFD modelling has become a convenient method for describing the characteristics of the pulverized coal combustion since it provides flow and thermal behaviour inside the equipment and reduces the amount of experimentation necessary to identify problems and to optimise the operating conditions. A review of CFD based models for co-firing coal and biomass was presented by Tabet and Gokalp (2015). They reported that the current CFD based model is capable of solving the complex interdependent processes like fluid flow, turbulence, heat transfer and heterogeneous and homogeneous chemical reactions involved in combustion. For modelling the turbulence characteristics of pulverized coal combustion, Kurose et. al. (2009) used both Reynolds Averaged Navier-Stokes approach (RANS) with the renormalization group $k-\varepsilon$ model and Large Eddy Simulation approach (LES). They found that regarding the prediction of the flow field, LES is superior to RANS simulation but LES approach consumes more computational cost. The result of RANS simulation can be improved by using a suitable turbulence model. Pallares et. al. (2009) reported that the realizable $k-\varepsilon$ model performs better than the standard $k-\varepsilon$ model in predicting swirling combustion flow. Mikulcic et. al. (2017) proposed the Eulerian-Lagrangian method for solving the multi-phase flow phenomena in a pulverized coal combustion furnace. They claimed that the proposed method provided better understanding of particle kinetics and distribution in the equipment. However, the study of the effect of various types of coal feeding pattern has not been investigated.

The objective of this work is to help industry to improve furnace efficiency by investigating the effect of coal feeding patterns on thermal efficiency and pollution emissions using CFD modelling with the realizable $k-\varepsilon$ turbulence model.

2. Mathematical model

In this work, the simulation assumes a continuous phase of reacting gases and a discrete phase of fuel particles setting the positions of the mass and heat sources while they travel immersed in the continuous phase. The continuous phase is a gas mixture, consisting of six species (volatiles, oxygen, carbon dioxide, water vapor, sulfur dioxide and nitrogen), whose composition is determined by solving the mass conservation equation as well as species conservation equations.

Governing equations

The general form of conservation equation of mass, momentum and energy are shown below.

$$\frac{\partial \rho}{\partial t} + \nabla \cdot (\rho \vec{v}) = S_m \quad (1)$$

$$\frac{\partial}{\partial t} (\rho \vec{v}) + \nabla \cdot (\rho \vec{v} \vec{v}) = -\nabla p + \nabla \cdot (\bar{\tau}) + \rho \vec{g} + \vec{F} \quad (2)$$

where $\bar{\tau}$ is the stress tensor, $\bar{\tau} = \mu \left[(\nabla \vec{v} + \nabla \vec{v}^T) - \frac{2}{3} \nabla \cdot \vec{v} \cdot \mathbf{I} \right]$, and \mathbf{I} is the unit tensor.

$$\frac{\partial}{\partial t} (\rho E) + \nabla \cdot (\vec{v} (\rho E + p)) = \nabla \cdot \left(k_{eff} \nabla T - \sum_j h_j J_j + (\bar{\tau}_{eff} \cdot \vec{v}) \right) + S_h \quad (3)$$

where k_{eff} is the effective conductivity, $\bar{\tau}_{eff}$ is the effective stress tensor (ANSYS, Inc., 2013) and J_j is the diffusion flux of the species. E in Eq(3) is defined as $E = h - \frac{p}{\rho} + \frac{v^2}{2}$ where h denotes sensible enthalpy, defined for incompressible flow as $h = \sum_j Y_j h_j + \frac{p}{\rho}$, and where $h_j = \int_{T_{ref}}^T C_{p,j} dT$, and T_{ref} is constant and taken as 298.15 K in this work. The source term, S_m , in Eq(1) is the mass added to the continuous phase from the dispersed phase during the process of devolatilization and char combustion. The force, \vec{F} , in Eq(2) arises from the interaction of the continuous with dispersed phase of the coal particles. The source term, S_h , in Eq(3) is provided by the net enthalpy formation rates from the species transport reaction including the heat of chemical reactions and radiation. The flow behaviour was simulated by solving the conservation of momentum equation under the RANS approach with turbulence model.

Turbulence model

In this work, the turbulence characteristics of the flow were modelled using the realizable $k-\varepsilon$ model. This realizable model has shown substantial improvements over the standard model in predicting the flow features including strong streamline curvature, vortices, and rotation. The turbulent kinetic energy, k , and its rate of dissipation, ε , are obtained from the following transport equation:

$$\frac{\partial}{\partial t} (\rho k) + \frac{\partial}{\partial x_j} (\rho k u_j) = \frac{\partial}{\partial x_j} \left[\left(\mu + \frac{\mu_t}{\sigma_k} \right) \frac{\partial k}{\partial x_j} \right] + G_k + G_b - \rho \varepsilon - Y_M + S_k \quad (4)$$

$$\frac{\partial}{\partial t} (\rho \varepsilon) + \frac{\partial}{\partial x_j} (\rho \varepsilon u_j) = \frac{\partial}{\partial x_j} \left[\left(\mu + \frac{\mu_t}{\sigma_\varepsilon} \right) \frac{\partial \varepsilon}{\partial x_j} \right] + \rho C_1 S_\varepsilon - \rho C_2 \frac{\varepsilon^2}{k + \sqrt{V \varepsilon}} + C_{1\varepsilon} \frac{\varepsilon}{k} C_{3\varepsilon} C_b + S_\varepsilon \quad (5)$$

G_k represents the generation of turbulence kinetic energy due to the mean velocity gradients and the Reynolds stress, and G_b represents the generation of turbulence kinetic energy due to buoyancy. Y_M denotes the contribution of the fluctuating dilatation in compressible turbulence to the overall dissipation rate. S_k and S_ε are source terms.

$$G_k = -\rho u'_i u'_j \frac{\partial u_j}{\partial x_i} \quad (6)$$

$$G_b = \beta g_i \frac{\mu_t}{Pr_t} \frac{\partial T}{\partial x_i} \quad (7)$$

$$Y_M = 2\rho\varepsilon M_t^2 \quad (8)$$

where Pr_t is the turbulence Prandtl number and g_i is the component of the gravitational vector in i -th direction, β is the coefficient of thermal expansion which is $\beta = -\frac{1}{\rho} \left(\frac{\partial \rho}{\partial T} \right)_p$. M_t is the turbulence Mach number given as

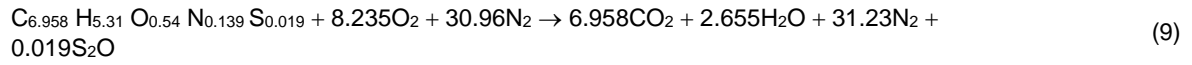
$M_t = \sqrt{\frac{k}{a^2}}$ and where $a = \sqrt{\gamma RT}$ is the speed of sound. The turbulent viscosity, μ_t is defined by $\mu_t = \rho C_\mu \frac{k^2}{\varepsilon}$,

$C_1 = \max\left[0.43, \frac{n}{n+5}\right]$, $n = S \frac{k}{\varepsilon}$, $S = \sqrt{2S_{ij}S_{ij}}$, $C_{1\varepsilon} = 1.44$, $C_2 = 1.9$, $\sigma_k = 1$, $\sigma_\varepsilon = 1.2$, and $C_{3\varepsilon}$ is equal 1 for buoyant shear layers for which the main flow direction is aligned with the direction of gravity. For buoyant shear layers that are perpendicular to the gravitational vector, it will be zero.

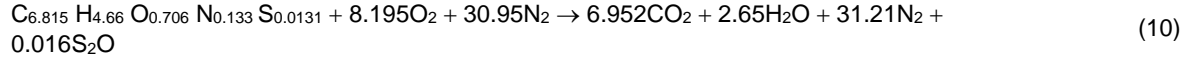
Combustion models

Three types of bituminous coal namely Coal A, B and C, were used in this work. Their properties are described in the next section (Table 1). The one-step global reaction mechanism of these coals, assuming complete conversion stoichiometric combustion, are

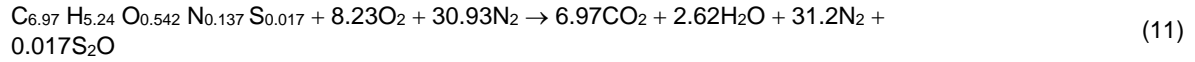
Coal A



Coal B



Coal C



The mixing and transport of chemical species, CO_2 , H_2O , N_2 and O_2 , are modelled by solving the conservation equations describing convection, diffusion, and reaction sources for each component species. The species transport equations are solved by predicting the local mass fraction of each species, Y_i , through the solution of a convection-diffusion equation for the i -th species. Since the mass fraction of the species must sum to unity, to minimize numerical error, the local mass fraction of the bulk species N_2 was predicted by subtraction. The species transport equation is

$$\frac{\partial}{\partial t} (\rho Y_i) + \nabla \cdot (\rho \vec{v} Y_i) = -\nabla \cdot J_i + R_i + S_i \quad (12)$$

where S_i is the rate of creation by addition from the coal particles dispersed, J_i is the diffusion flux of species i , which accounts to the concentration gradients and R_i is the net rate of production of species i by chemical reaction. The reaction rate in the source term of this equation, caused by the turbulence-chemistry interaction, is computed by the eddy-dissipation model. The equations describing these variables can be found in ANSYS, Inc. (2013).

3. Computational method

The three-dimensional numerical simulation of a 1,434 MW pulverised coal combustion furnace located in BLC Power Station was considered. The combustion and thermal flow behaviour inside this furnace for six cases of coal feeding patterns with equivalent coal feed rate were investigated.

Furnace and burner configuration

The schematic diagram of the computational model is presented in Figure 1. The burner has two inlets, one for air and the other for air and fuel. The primary air enters the burner with coal in the inner duct with 0.25 m radius as shown in Figure 1, and the secondary air enters around the outside periphery of the primary air and coal, with 0.5 m total internal radius. There are three burners located vertically in the middle of the furnace side-wall.

Coal properties

The co-firing combustion of three types of bituminous coal used in BLC Power Station, Thailand, were simulated. Their proximate and ultimate properties are summarised in Table 1. These coals have a low content of sulphur but a high heating value. Coal type A has higher fixed carbon content, higher oxygen content and lower ash content than type A and C. In this study, a coal particle is assumed to be spherical in shape. The coal

particle density is $1,390 \text{ kg}\cdot\text{m}^{-3}$. The coal particles are in the range of $70\text{-}200 \mu\text{m}$ and an average diameter is $134 \mu\text{m}$. The coal particle distribution is defined as Rosin-Rammler distribution (RRD) with a spread parameter of 4.53, the detail of RRD being given by Al-Abbas et. al. (2012).

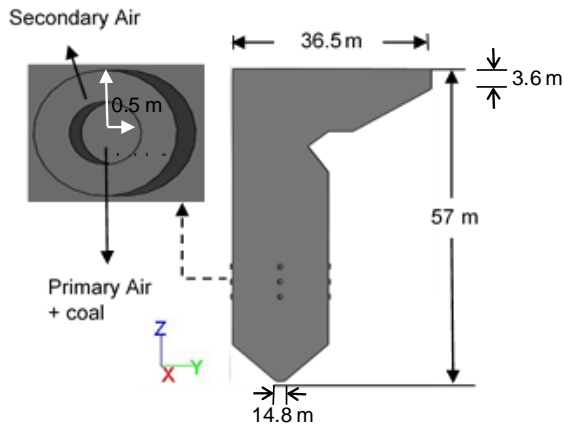


Figure 1: Schematic of the boiler furnace used in this computational model.

Table 1: Fuel properties used in this study.

Coal type	Ultimate analysis (% wt)			Coal type	Proximate analysis (% wt)		
	A	B	C		A	B	C
Carbon	83.49	81.76	83.63	Volatile	28.61	25.84	28.41
Hydrogen	5.31	4.66	5.24	Fixed carbon	47.70	50.05	48.04
Oxygen	8.64	11.30	8.68	Ash	14.50	9.66	12.88
Nitrogen	1.95	1.86	1.92	Moisture	9.20	14.46	10.67
Sulfur	0.62	0.42	0.53				
GCV($\text{MJ}\cdot\text{kg}^{-1}$)	26.04	25.18	26.12				

3.3 Cases considered for CFD modelling

In the present study, six different cases of coal feeding patterns have been considered to investigate the thermal performance and the gaseous emissions under the equivalent coal feed rate. Six different patterns are shown in Figure 2. Each pattern is different in the feeding position of each coal type, (Coal A, B and C).

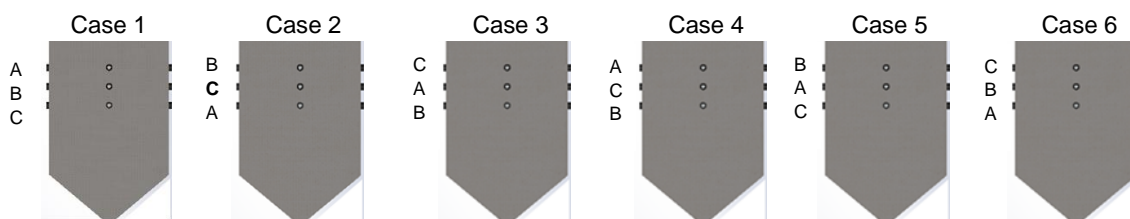


Figure 2: Coal feeding patterns.

3.4 Boundary conditions and numerical technique

Mass flow rate and inlet conditions are applied at all inlets in the burner. A pressure outlet boundary condition is applied at the outlet. The furnace walls are stationary with no-slip conditions applied on the wall surface. The wall temperature is set to be constant. The boundary condition is assumed as follows: excess air percentage is 20%, coal feed flow rate is $0.24 \text{ kg}\cdot\text{s}^{-1}$ for all types of coal, primary air feed flow rate is $1 \text{ kg}\cdot\text{s}^{-1}$, secondary air feed flow rate is $1 \text{ kg}\cdot\text{s}^{-1}$, outlet pressure is 101.325 kPa , wall temperature is $1,000 \text{ K}$, specific heat for all types of coal is $1,680 \text{ J}\cdot\text{kg}^{-1}\cdot\text{s}^{-1}$ and thermal conductivity is $0.033 \text{ W}\cdot\text{m}^{-1}\cdot\text{K}^{-1}$. All the simulations were carried out in the commercial software FLUENT 12.0.7, which is based on the Finite Volume Method (FVM) to discretise the governing equations in terms of the algebraic equations. These discretised equations were solved using the

Semi-Implicit Method for Pressure-Linked Equations (SIMPLE) algorithm developed by Patankar (1980). The computational mesh contains 900,000 unconstructed tetrahedral elements, which provide the grid independence solution.

4. Simulation results and discussion

The numerical results from the computational model used in this work were validated with the experimental work on pulverized coal combustion of Lu (2008). The calculated data of the temperature and the percent of CO₂ and SO₂ at the exit of the furnace shows a close correlation with the experimental data with only minimum deviation of 3.75 % on average in the temperature profile. The simulated velocity and temperature fields are presented in Figures 3 and 4. Figure 3a depicts the main and inert burning areas where the fuel mixes with the oxidizer, which leads to a higher flame temperature compared to the other areas inside the equipment.

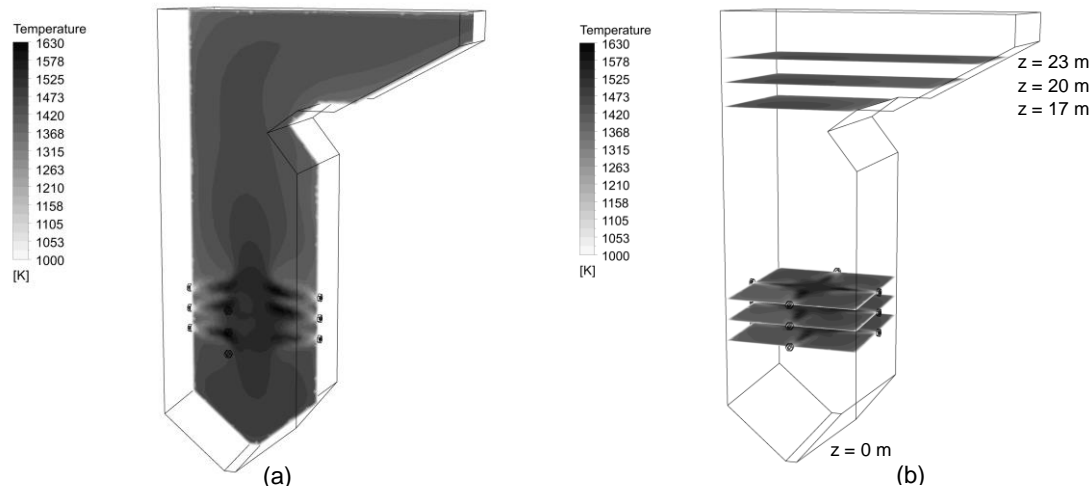


Figure 3: The temperature contour of Case 2 (BCA); (a) temperature distribution in vertical plane and (b) temperature distribution in horizontal plane at the feed positions of coal and at the heat exchanger tube area ($z = 17$ m, 20 m and 23 m).

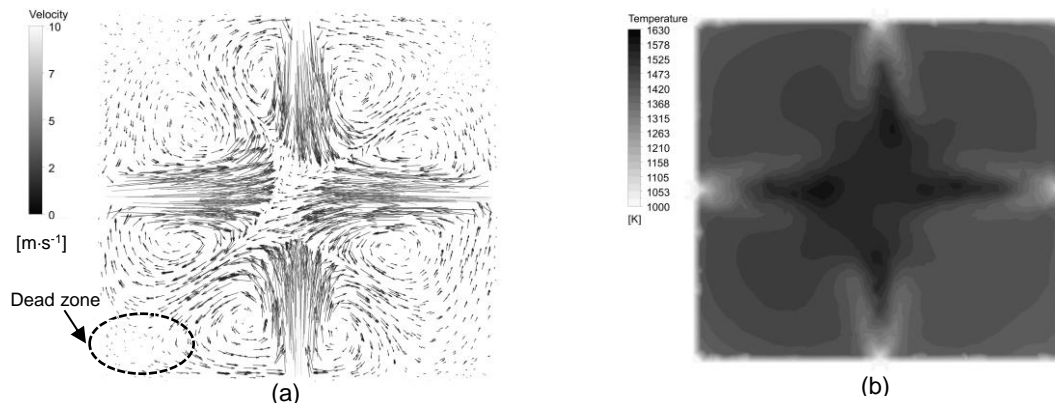


Figure 4: The thermal and flow behaviour of Case 2 (BCA); (a) velocity vector ($m \cdot s^{-1}$) and (b) chamber temperature (K) at the feed position of C type coal.

Compared to the main reaction zone, a decrease in the flue gas temperature was observed in the upper zone. Figure 4 shows the recirculation characteristic in the main reaction zone which provides the better mixing characteristic of fuel, leading to improved combustion performance. However, the low temperature areas were also observed where no combustion takes place (Dead zone). More areas of dead zone will cause lower thermal efficiency because the coals will move downward and combust in the bottom area of the furnace meaning that the high temperature is obtained here instead of the heat transfer area. The flue gas temperature in the middle of the furnace at the planes $z = 17$ m, 20 m and 23 m from the bottom of the equipment, where the heat exchanger tubes are located, for six cases are shown in Figure 5a. It was found that Case 2 (BCA) and Case 5

(BAC) gave higher temperature at heat transfer regions for steam production than the other cases, and Case 2 (BCA) gave the maximum temperature. This indicates that feeding coal with a higher fixed carbon content at the top position yielded higher thermal efficiency. It also released minimum flue gases (SO_2 , CO_2), which was more environmentally friendly, as can be seen in Figures 5b and 5c. These graphs show the mass flow rate of CO_2 and SO_2 at the furnace exit. Feeding coal with high sulfur and carbon contents at the bottom burner helps to reduce CO_2 and SO_2 emissions.

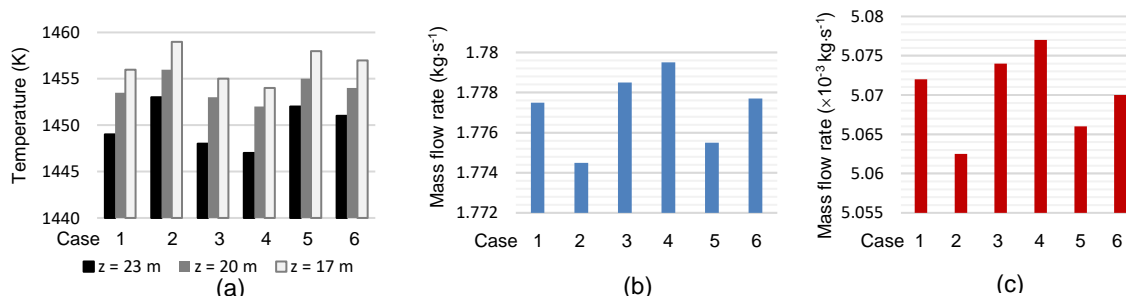


Figure 5: The flue gas temperature (K) in the middle of the furnace at the plane $z = 17$ m, 20 m and 23 m from the bottom of the equipment (a), the mass flow rate of CO_2 ($\text{kg}\cdot\text{s}^{-1}$) at the furnace exit (b) and the mass flow rate of SO_2 ($\times 10^{-3} \text{kg}\cdot\text{s}^{-1}$) at the furnace exit (c).

5. Conclusions

The effect of coal feeding patterns on combustion efficiency in a 1,434 MW pulverised coal combustion furnace using CFD technique has been investigated. The simulation results provided important combustion characteristics such as temperature distributions and flow behaviour in the reaction and dead zones, which offers an understanding of the coal firing process in the furnace. The pulverized coal combustion characteristics can be changed considerably with slight variation in the species compositions in volatile matter. The essence of this study is that the coal feeding pattern can improve furnace efficiency and reduce pollution emissions. The results gained from this study can help the industry to improve furnace efficiency by feeding coal at an optimised pattern. Future work will include NO_x and CO predictions.

Acknowledgments

The author is grateful to BLCP Power Station, Thailand and Assoc. Prof. Dr. Suneerat Fukuda for the furnace information in this study, and wishes to acknowledge the assistance of Laotongsarn, N. and Kamkhantee, N. for the simulation process.

References

- Al-Abbas A. H., Naser J., Dodds D., 2012, CFD Modelling of AIR-FIRED AND OXY-FUEL COMBUSTION IN A LARGE-SCALE FURNACE AT Loy Yang A Bown Coal Power Station, Fuel, 102, 646–665.
- ANSYS, Inc., 2013, Ansys Fluent Theory Guide, Canonsburg, USA.
- Kurose R., Watanabe H., Makino H., 2009, Numerical Simulations of Pulverized Coal Combustion, KONA Powder and Particle Journal, 27, 144–156.
- Lu Q., 2008, Pulverized Coal Combustion and NO_x Emissions in High Temperature Air from Circulating fluidized bed, Fuel Processing Technology, 89, 1186–1192.
- Mikulcic H., Berg E.V., Wang X., Vujanovic M., Tan H., Duic N., 2017, Using an Advanced Numerical Technique for Improving Pulverized Coal Combustion Inside an Industrial Furnace, Chemical Engineering Transaction, 61, 235–246.
- Pallares J., Gil A., Cortes C., Herce C., 2009, Numerical Study of Co-Firing Coal and Cynara Cardunculus, in a 350MWe Utility Boiler, Fuel Processing Technology, 90, 1207–1213.
- Patankar S. V., 1980, Numerical Heat Transfer and Fluid Flow, Hemi-Sphere Publishing Corporation, Taylor and Francis Group, New York, USA.
- Tabet F., Gokalp I., 2015, Review on CFD based Models for Co-firing Coal and Biomass, Renewable and Sustainable Energy Reviews, 51, 1101–1114.
- Wen X., Wang H., Luo Y., Luo K., Fan J., 2017, Numerical Investigation of the Effect of Volatile Matter Composition and Chemical Reaction Mechanism on Pulverized coal Combustion Characteristics, Fuel, 210, 685–704.